ORIGINAL ARTICLE

Development of a multimodal kidney age prediction based on automatic segmentation CT image in patients with normal renal function

Zuoxian Hou [1], Gumuyang Zhang[2], Yixin Ma[1], Peng Xia[1], Xiaoxiao Shi[1], Wenlong She[3], Tianzuo Zhao[3], Hao Sun[2], Zhengguang Chen[3] and Limeng Chen[1]

[1]Department of Nephrology, Peking Union Medical College Hospital, Chinese Academy of Medical Sciences, Beijing, China, [2]Department of Radiology, Peking Union Medical College Hospital, Chinese Academy of Medical Sciences, Beijing, China and [3]Department of Radiology, Dongzhimen Hospital, Beijing University of Chinese Medicine, Beijing, China

Correspondence to: Limeng Chen; E-mail: chenlimeng@pumch.cn; Hao Sun; sunhao_robert@126.com

ABSTRACT

Background. For decades, description of renal function has been of interest to clinicians and researchers. Serum creatinine (Scr) and estimated glomerular filtration rate (eGFR) are familiar but also limited in many circumstances. Meanwhile, the physiological volumes of the kidney cortex and medulla are presumed to change with age and have been proven to change with decreasing kidney function.

Methods. We recruited 182 patients with normal Scr levels between October 2021 and February 2022 in Peking Union Medical College Hospital (PUMCH) with demographic and clinical data. A 3D U-Net architecture is used for both cortex and medullary separation, and volume calculation. In addition, we included patients with the same inclusion criteria but with diabetes (PUMCH-DM test set) and diabetic nephropathy (PUMCH-DN test set) for internal comparison to verify the possible clinical value of "kidney age" (K-AGE).

Results. The PUMCH training set included 146 participants with a mean age of 47.5 ± 7.4 years and mean Scr 63.5 ± 12.3 μmol/L. The PUMCH test set included 36 participants with a mean age of 47.1 ± 7.9 years and mean Scr 66.9 ± 13.0 μmol/L. The multimodal method predicted K-AGE approximately close to the patient's actual physiological age, with 92% prediction within the 95% confidential interval. The mean absolute error increases with disease progression (PUMCH 5.00, PUMCH-DM 6.99, PUMCH-DN 9.32).

Conclusion. We established a machine learning model for predicting the K-AGE, which offered the possibility of evaluating the whole kidney health in normal kidney aging and in disease conditions.

LAY SUMMARY

We established a multimodal machine learning method to estimate the "kidney age" (K-AGE) for evaluating the whole renal health status. We recruited 182 patients with normal serum creatinine levels from Peking Union Medical

College Hospital for data acquisition and model training. First, we used semantic segmentation (a deep learning method) to auto-segment the kidney volume into different regions (cortex and medulla). Then we trained a multimodal machine learning model applying the combination of volumes and clinical characteristics as input features, and patients' chronological age as output feature. Differences in K-AGE prediction (K-AGE delta) were found between various types of computed tomography (CT) images (contrast-enhanced CT and non-contrast-enhanced CT). K-AGE delta also differed between the control group, diabetes mellitus group and diabetic nephropathy group.

INTRODUCTION

For decades, clinicians and researchers have tried hard to define a suitable way to describe the overall kidney health status of a patient. Unfortunately, after one and half centuries [1], serum creatinine (Scr) [2] or the estimated glomerular filtration rate (eGFR) computed by formulas based on Scr [3–5] are still the most commonly used markers of GFR since 1999. Although the bias of Scr affected by muscle mass and metabolic status [6] can be corrected by eGFR, the eGFR formula depends on data from specific populations with limitation in some cases, for example, in overweight or elderly populations. Chuah *et al.* observed that eGFR measurement in patients undergoing obesity surgery might not be accurate because of creatinine reduction accompanied by muscle-mass reduction [7], which is consistent with the report that both body adiposity index and visceral adiposity index would influence the calculation of eGFR [8, 9]. In addition, pathological renal structural changes usually result from kidney disease caused by various etiologies, such as glomerular sclerosis, interstitial fibrosis and tubular atrophy [10], usually coupled with a decline in GFR [11–14]. Furthermore, due to the compensatory capacity of the kidney, sometimes the structural damage to the kidney is noted as more sensitive evidence than an elevation of serum creatinine. Meanwhile, kidney aging correlates well with kidney volumes and function decreasing [15]. Therefore, it is an urgent task to define a more comprehensive method to assess the overall condition of kidney structure and function.

Recently, automatic kidney segmentation techniques combining kidney images derived from magnetic resonance (MR) imaging or computed tomography (CT) and artificial intelligence algorithms is developed, which is a novel fully automated method to separately segment each kidney cortex and medulla in contrast-enhanced CT images [16]. These new techniques offer the possibility of evaluating the whole kidney health status in combination with clinical data. Similar strategies are also successfully applied in the brain and heart [17, 18].

In this study, we included as the study cohort populations whose Scr is between normal ranges and without significant kidney structural defects. Based on an auto-segmentation algorithm on either standard CT or contrasted-enhanced CT, we developed a prediction model for the "kidney age" (K-AGE) of populations involving kidney structure information. Clinical characteristics were also collected to eliminate its possible distraction on prediction. The difference between the actual physiological age and the K-AGE was used to verify the model's accuracy and was also considered a measure of accelerated (or decelerated) kidney aging.

MATERIALS AND METHODS

Study cohort

We included patients with normal Scr levels and abdominal contrast-enhanced CT images between October 2021 and February 2022 in Peking Union Medical College Hospital (PUMCH dataset). The inclusion criteria were: (i) patients aged >35 years, (ii) no reported history of kidney disease, (iii) complete laboratory results including Scr, albumin (Alb) and electrolytes, (iv) normal Scr levels, (v) received abdominal contrast-enhanced CT scan and (vi) no anatomic abnormalities of kidneys revealed by CT scan. All CT exams were acquired on a 256-slice CT scanner (Discovery CT 750 HD, GE Healthcare), a dual-source dual-energy CT scanner (Somatom Definition Flash, Siemens Healthcare) or an Aquilion ONE Genesis scanner (Canon Medical Systems). Images files of CT scan were firstly exported as Dicom format, then transformed into NIFTI format (through Python code) for further operation. The exclusion criteria were: (i) CT images failed to be transformed into NIFTI format, and (ii) incomplete laboratory results or patient information (Fig. 1). In addition, we included patients with the same inclusion criteria but with diabetes (PUMCH-DM test set) and diabetic nephropathy (PUMCH-DN test set) for internal comparison to verify the possible clinical value of K-AGE. Data from DongZhiMen Hospital (DZMH test set) were used as separate external validation sets to evaluate model generalizability. This study was approved by the Institutional Review Boards of PUMCH (S-K1975). The informed consent was waived since de-identified images were used.

Data collection

We collected the clinical data from the medical records, including age, gender, height, weight, current smoker and intake of alcohol, and lab data included Scr, sodium (Na), Alb, etc. Body mass index (BMI) was calculated as weight (kg)/height $(m)^2$ and eGFR was calculated using the Chronic Kidney Disease Epidemiology Collaboration (CKD-EPI) equation [19]. Selected types of data in the PUMCH dataset were randomly chosen according to the statistical analysis and separated into a training set (PUMCH training set, 80%) and a test set (PUMCH test set, 20%) following equal age distribution. Data augmentation was applied by adding random Gaussian noise to the PUMCH training set to reduce the prediction error because of the unbalanced distribution of patient age.

Image data annotation

We annotated the imaging data to create the ground truth and to build the automatic segmentation algorithm. The standard
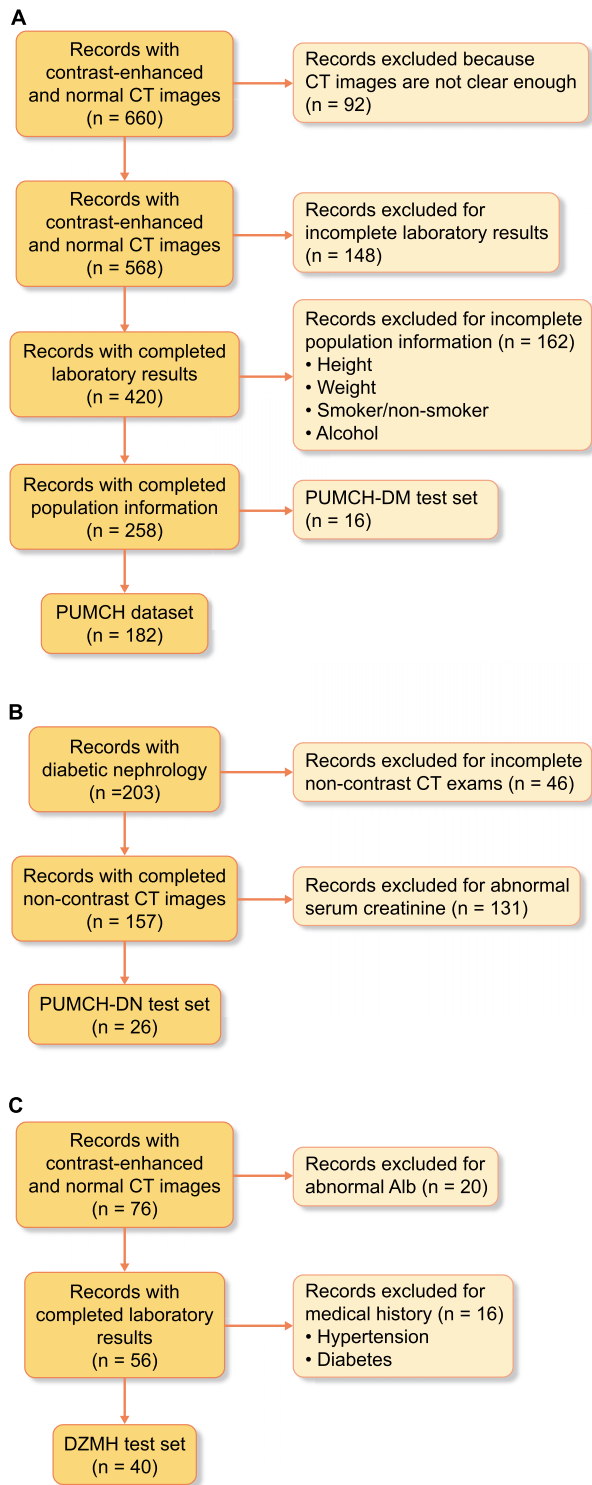
A

```
Records with                    Records excluded because
contrast-enhanced               CT images are not clear enough
and normal CT images            (n = 92)
(n = 660)
        │
Records with                    Records excluded for
contrast-enhanced               incomplete laboratory results
and normal CT images            (n = 148)
(n = 568)
        │
Records with completed          Records excluded for incomplete
laboratory results              population information (n = 162)
(n = 420)                       • Height
                                • Weight
                                • Smoker/non-smoker
                                • Alcohol
        │
Records with completed          PUMCH-DM test set
population information           (n = 16)
(n = 258)
        │
PUMCH dataset
(n = 182)
```

B

```
Records with                    Records excluded for incomplete
diabetic nephrology             non-contrast CT exams (n = 46)
(n =203)
        │
Records with completed          Records excluded for abnormal
non-contrast CT images          serum creatinine (n = 131)
(n = 157)
        │
PUMCH-DN test set
(n = 26)
```

C

```
Records with                    Records excluded for
contrast-enhanced               abnormal Alb (n = 20)
and normal CT images
(n = 76)
        │
Records with                    Records excluded for
completed laboratory            medical history (n = 16)
results                         • Hypertension
(n = 56)                        • Diabetes
        │
DZMH test set
(n = 40)
```

Figure 1: (**A**) Patient flow chart for PUMCH dataset. (**B**) Patient flow chart for PUMCH-DN dataset. (**C**) Patient flow chart for DZMH dataset.

CT images were annotated by a senior radiologist with 5 years of experience using ITK-SNAP (version 3.8). First, the sub-region is manually identified from the axial plane to include both kidneys. Then, we used active contour evolution for kidney segmentation based on intensity value thresholds in the sub-region (Supplementary data, Fig. S1) [16].

The design of automatic segmentation algorithms

The prediction of K-AGE contained two steps with different algorithms (Fig. 2). First was automatic kidney segmentation with two deep learning methods for automatic kidney segmentation. A modified U-Net architecture [16] (named U-NET-Con) was applied to auto-segment the contrast-enhanced CT images of kidneys into four classes (right cortex, right medulla, left cortex and left medulla) for volume and ratio calculation of each part. Then, we developed another U-Net architecture (named U-NET-STD) to automatically segment standard CT images for volume calculation of the right and left kidneys in verification and comparison (Fig. 3).

The design of the K-AGE prediction algorithm

We first designed a stacking regressor for K-AGE prediction based on the combination of clinical data and images by the machine-learning model, which consisted of a Random Forest, an Extra Trees and a linear regression algorithm. In the PUMCH training set, different initial weights were randomly batched to train the stacking regressor (100 times). Through 100 repetitions, the final test result was described as the weighted average value derived in the test sets of PUMCH and DZMH. The prediction performance was measured by the mean absolute error (MAE) between the predicted K-AGE and the actual physiological age. The predictions were defined to be accurate if the true age was in the 95% confidence interval of the predicted K-AGE. Finally, various models were trained based on different combinations of image data from the auto-segmentation of CT images (Fig. 2), then the prediction results of K-AGE from the three models were compared.

Statistical analysis

Categorical variables were shown as frequency and percentage, and continuous variables as mean values with standard deviation were analyzed. We used the one-way analysis of variance (ANOVA) analysis to compare continuous variables with the normal distribution and the chi-squared test to compare the proportion of categoric variables. The multi-linear regression was used to describe age and kidney volume correlations, with a *P*-value of <.05 considered statistically significant. The relationship between clinical characteristics and kidney volume of each part was illustrated by the "regplot" function in Python library (Version 3.8).

RESULTS

Clinical characteristics and auto-segmentation kidney volume

The study included 182 participants with CT or contrast-enhanced CT images from PUMCH and the training set participants (146) with a mean age of 47.5 ± 7.4 years, 58.9% female and mean Scr 63.5 ± 12.3 μmol/L; the PUMCH test set ($n = 36$) and DZMH external validation set ($n = 40$) had similar mean age, female percentage and mean Scr levels, without significant difference (Table 1). Auto-segmentation kidney volume estimated by U-NET-Con indicated no significant difference among the total kidney volume, both sides kidney cortex and medullar volume among the PUMCH training set, PUMCH test set and DZMH test set (Table 1).
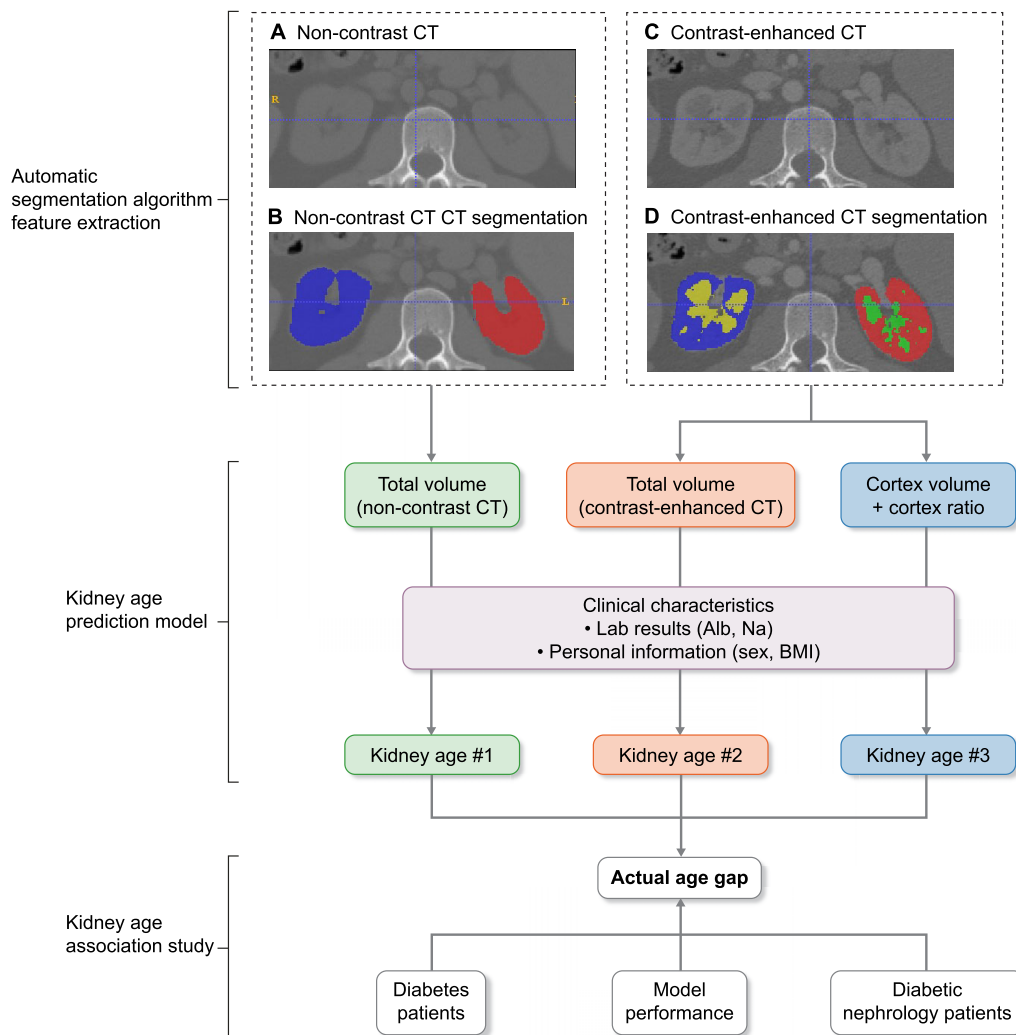
Figure 2: Flow chart shows model performance comparison between various types of the automatic segmentation algorithm.

Correlation between auto-segmentation kidney volumes and age

Age was significantly associated with the total kidney volume and cortical volume obtained by automated segmentation in two models with different adjusted parameters (only gender, or BMI, Alb, Na, smoking status, alcohol intake and Scr), neither kidney medullary volume (Table 2). Participants with higher eGFR (eGFR >110) had a relatively larger cortex volume than those with lower eGFR (eGFR <110). Meanwhile, the cortex volume of participants with high BMI (BMI >24) attenuated more slowly than those with BMI <24 (Supplementary data, Fig. S2).

Performance of automatic segmentation and K-AGE

We obtained a similar automated segmentation by the CT and enhanced CT in the PUMCH test set (Fig. 4). For segmented kidneys, the volume differences between CT and enhanced CT in both side kidneys were not evident ($P < .01$, Fig. 5).

In the U-NET-Con segmentation algorithm, the total prediction accuracy of K-AGE prediction from the cortical volume and ratio is 91.7% with MAE 3.46 ($r = 0.81$, $P < .01$), while 83.3% of the whole kidney volume had a slightly higher MAE 5.16 ($r = 0.57$, $P < .01$). There was a similar performance of the total kidney volume from U-NET-STD (83.3%, MAE = 5.00, $r = 0.56$, $P < .01$, Fig. 6a–c).

The total prediction accuracy of K-AGE prediction in the DZMH test set, based on the cortical volume and ratio from the U-NET-Con segmentation algorithm, is 90.0% with MAE as 3.94 ($r = 0.80$, $P < .01$). We observed less prediction accuracy (82.5%) and a higher MAE (5.39, $r = 0.46$, $P < .01$) based on the total kidney volume in U-NET-Con and U-NET-STD of 82.5% (MAE = 4.79, $r = 0.51$, $P < .01$, Fig. 6d–f).

Performance of K-AGE in diabetes patients

By the U-NET-STD segmentation algorithm, the MAE of K-AGE prediction in diabetic nephropathy is the highest in the PUMCH-DN test set (9.32, $r = 0.32$, $P = .11$), followed by the PUMCH-DM
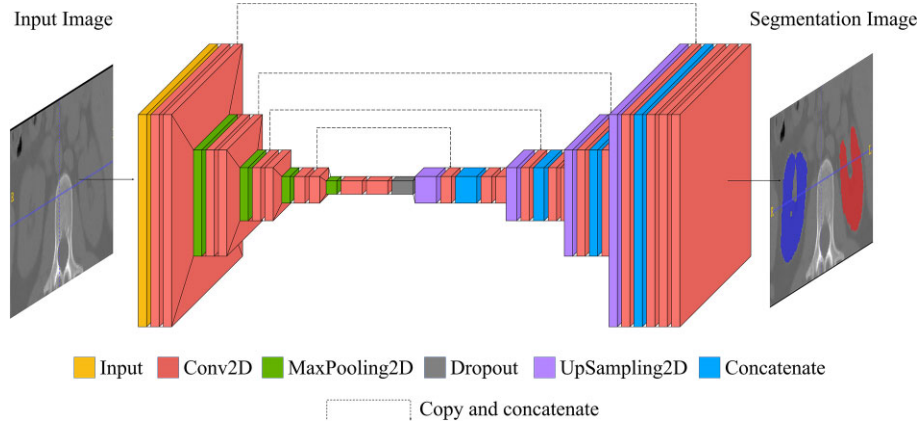
Figure 3: Architecture of U-NET-STD for non-contrasted enhanced CT image segmentation.

Table 1: Clinical characteristics of study subjects for the training validation and test sets considered in this study.

Clinical characteristics	PUMCH training set (N = 146)	PUMCH test set (N = 36)	DZMH test set (N = 40)	P
Age (years)	47.5 ± 7.4	47.1 ± 7.0	50.2 ± 7.5	.103
Sex, n (%)				
Men	60 (41)	17 (47)	15 (37)	.857
Women	86 (59)	19 (53)	25 (63)	
Height (cm)	166.30 ± 7.13	167.00 ± 7.49	164.16 ± 5.80	.133
Weight (kg)	63.50 ± 10.85	65.61 ± 12.22	63.59 ± 10.92	.586
BMI (kg/m^2)	22.90 ± 3.26	23.44 ± 3.64	23.58 ± 3.58	.432
Alb (g/L)	41.62 ± 5.11	41.91 ± 4.56	39.39 ± 3.83	.025
Na (mmol/L)	139.77 ± 2.34	139.77 ± 1.79	139.80 ± 3.25	.998
Smoking, n (%)	35 (24%)	11 (31%)	8 (20%)	.703
Alcohol, n (%)	39 (27%)	11 (31%)	7 (18%)	.552
Scr (μmol/L)	63.47 ± 12.31	66.91 ± 12.97	61.28 ± 10.69	.127
eGFR (mL/min/1.73 m^2)	107.57 ± 9.31	105.89 ± 10.53	107.36 ± 7.49	.617
Volume (mL)				
Right cortex	100.50 ± 20.31	103.34 ± 24.14	96.47 ± 23.04	.368
Right medulla	41.26 ± 10.40	45.94 ± 15.01	42.65 ± 11.42	.089
Left cortex	101.51 ± 20.57	103.80 ± 24.93	101.33 ± 25.19	.846
Left medulla	43.83 ± 10.84	45.82 ± 19.98	46.65 ± 11.59	.398

Values are presented as mean (standard deviation) unless stated otherwise.

eGFR was calculated by CKD-EPI equation.

P-value was calculated by the one-way ANOVA test for continuous variables and a chi-square test for categorical variables.

test set (6.99, r = 0.44, P = .09), and smallest in PUMCH test set (5.00, r = 0.56, P < .01, Fig. 7).

DISCUSSION

In this research, we first developed deep learning algorithms based on kidney CT images to complete the comprehensive and automated assessment of the renal structure, a stable K-AGE prediction model combined with the images and clinical data. Additionally, we applied this multimodal method to clinical systems to reveal structure abnormalities and detect potential kidney disease.

In our study, we observed decreased kidney cortex volume and increased medulla volume with age, which is consistent with the decrease in total kidney volume published before [14, 15]. Kidney cortex and medulla volume both show a positive correlation with gender, height, BMI and eGFR, which matched

the conclusion of the earlier research [16]. Automatic segmentation in the kidney has been of interest for years, spanning various imaging systems and segmentation algorithms. Cai *et al*. proposed a semi-automatic segmentation method of the renal cortex and medulla based on dynamic MR images in pigs [20]. Couteaux *et al*. trained an ensemble of fully convolutional networks (2D U-NET) to aggregate their prediction at test time to perform the segmentation [21]. Li *et al*. presented an automatic renal cortex segmentation approach using implicit shape registration and novel multiple surfaces graph search based on a hierarchy system [22]. In this study, a novel method of standard CT segmentation is established and compared with a published contrasted-enhanced CT segmentation method. Considering total kidney volume, U-NET-Con has a similar kidney segmentation effect to U-NET-STD, with prediction of K-AGE by total kidney volume from these two segmentation methods being without significant difference. However, U-NET-Con can

Table 2: Multiple linear regression coefficients between age and kidney volumes obtained by automated segmentation.

Independent variables	Model 1			Model 2		
	Coef	P	(95% CI)	Coef	P	(95% CI)
Total volume	−0.042	<.001	−0.062 to −0.022	−0.039	<.001	−0.031 to 0.004
Cortex volume	−0.076	<.001	−0.100 to −0.052	−0.074	<.001	−0.058 to −0.013
Medulla volume	0.011	.642	−0.035 to 0.057	0.021	.393	−0.008 to 0.064

Model 1 was adjusted for gender only.
Model 2 was adjusted for gender, BMI, Alb, Na, smoking status, alcohol intake, Scr.
Coef, coefficient; CI, confidence interval.
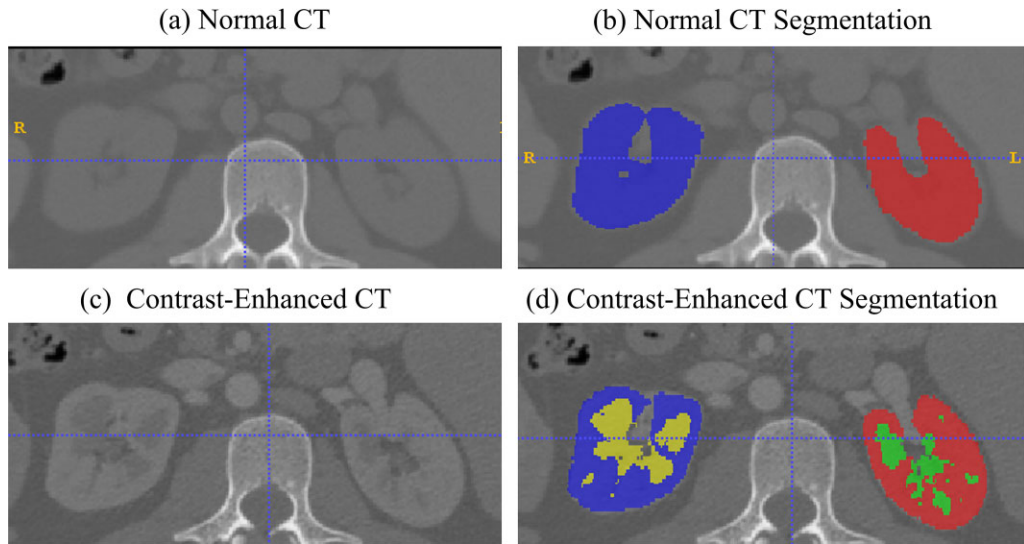
Figure 4: An example of automated segmentations for standard CT and contrast-enhanced CT segmentation results.

offer detailed information about kidney cortical and medullary information for a better prediction performance of K-AGE.

K-AGE aims to describe the total health status of the kidney in both kidney function and structure to help acknowledge patients' condition more comprehensively. Both structural and functional changes are related to the human aging process in systemic organs, such as the kidney, liver, brain and heart. Mclean *et al*. revealed significant age-related thickening of the sinusoidal endothelium with loss of fenestrations of the liver, which might impair the transfer by diffusion of substrates such as oxygen and drugs [23]. Ritchie *et al*. show that brain volume declines with age in the geriatric population, while white matter volumes are informative about cognitive decline with age [24]. Horn showed that aging-induced myocyte cell necrosis or apoptosis leads to hypertrophy of the remaining myocytes [25]. Therefore, we want to unite the structural and functional changes to evaluate the overall health status of the kidney. Coincidentally, this multimodal method has been applied in the prediction of "heart age." In their interpretable biological estimation model, cardiovascular magnetic resonance radionics measures the ventricular shape and myocardial characters [26]. As we know, kidney physiological changes and pathological implications vary with age [10]. In this study, we take the lead in raising the concept of K-AGE as an intermediate variable and establish an estimation model utilizing multimodal renal information (including auto-segmentation contrast-enhanced and standard CT images and clinical data in subjects without kidney diseases). The stability of the method made it possible to dig into the potential relationship between structural and functional changes with multi-center validation, to verify different effects on K-AGE prediction from CT with or without contrast enhancement, and finally to describe the overall health status of the kidney.

Although the Scr is within the normal range, patients with or without diabetes and diabetic nephropathy perform differently in the K-AGE prediction. Patients with diabetes have a relatively larger K-AGE variance than non-diabetic patients, and there was more variance in diabetic nephropathy patients. This may reveal the effects of potential kidney diseases on imaging examination. Though the predicted K-AGE performs similarly between standard CT and contrast-enhanced CT, contrast-enhanced CT is still superior in the calculation of cortex volume and ratio. However, contrast-induced kidney injury still accounts for about 11% of all cases of hospital-acquired acute kidney injury [27], and standard CT has better popularity in elder patients with renal insufficiency.

There are also some limitations to the prediction model. Firstly, K-AGE prediction performance is limited by the sample size, especially in an aged population with relatively normal renal function. As a retrospective study, we did not involve enough diabetic patients who had normal renal function and normal blood pressure at the same time. In a future prospective study, more diabetic patients should be included. Secondly, it could be optimized with more input clinical and imaging features for
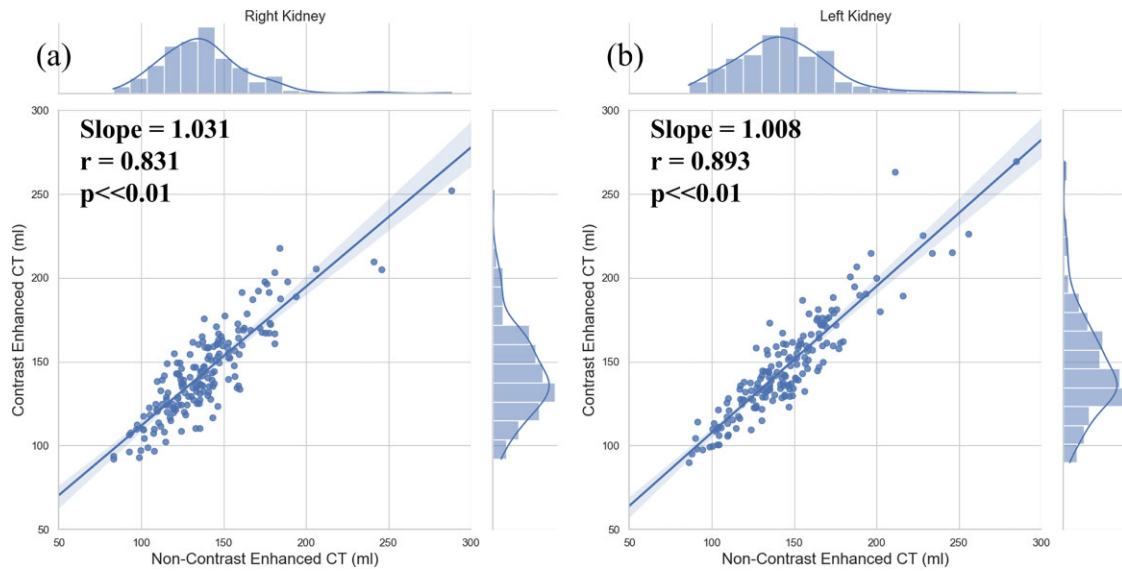
Figure 5: High correlation and agreement for volume measurements obtained from contrast-enhanced CT and standard CT.
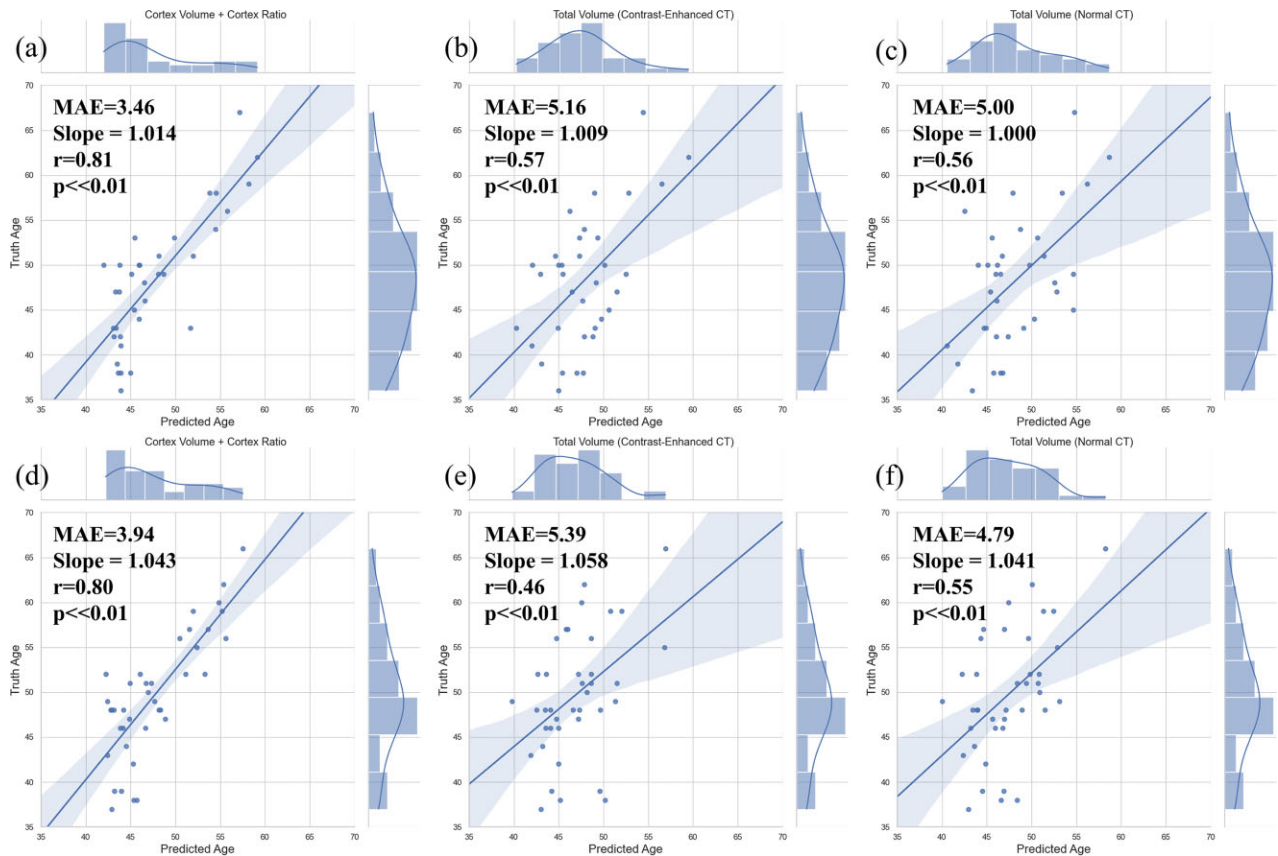

Figure 6: The agreement of K-AGE and actual physiological age in the test set obtained from contrast-enhanced CT and standard CT automatic segmentation in PUMCH test set and DZMH test set.

model training, such as 24-h urine protein, high-density lipid cholesterol [15] and kidney stiffness measurement [28, 29]. Finally, as a cross-sectional study, we could not confirm the K-AGE in predicting the endpoint of the patients during the follow-up visits.

Besides CT, other techniques are also used to evaluate the kidney structure. Ultrasound evaluation is a noninvasive imaging technique to assess kidney structure. However, the challenge is rooted in the scarcity of standardized ultrasound image datasets for deep learning training, attributable to the common
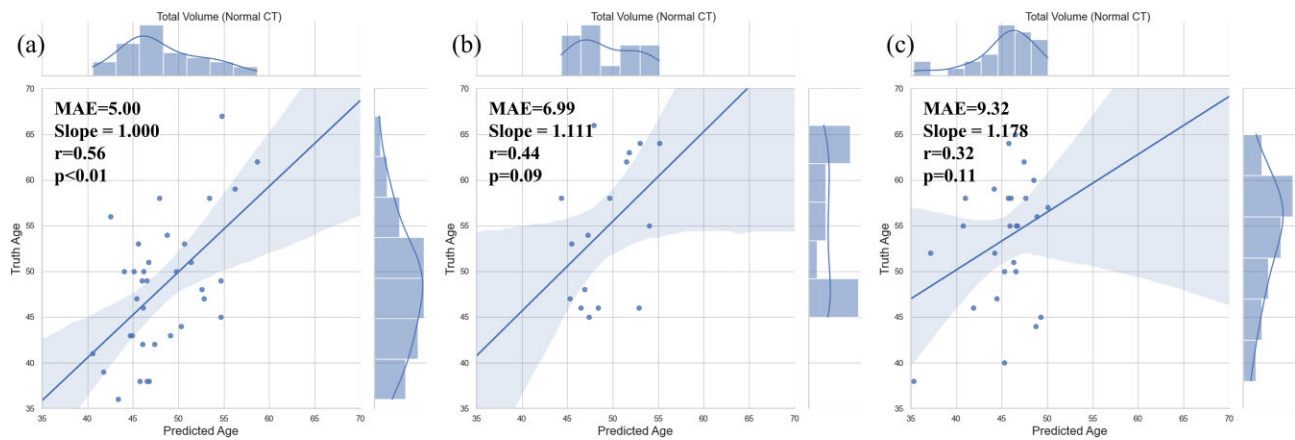
Figure 7: The K-AGE prediction in PUMCH, PUMCH-DM and PUMCH-DN test sets applying U-NET-STD segmentation algorithm in non-contrast CT images.

practice of sonologists in China who capture and diagnose ultrasound images concurrently, without preserving high-quality data. A future prospective study with standard records would benefit the deep learning training process. MR evaluation could also describe the kidney structure boundary similarly, but kidney MR evaluation is relatively underutilized in China, and our preliminary results based on public databases suffer from limited spatial resolution, which compromises the imaging quality (Supplementary data, Fig. S3). In addition, patients with different diseases, eGFR and renal structure abnormality should be involved as input features for further optimizing the prediction model. The gap between K-AGE and true age will help to indicate potential kidney disorders and predict prognosis.

CONCLUSION

We developed a segmentation algorithm based on CT images using published and self-developed algorithms that can accurately assess the kidney structure. Combined with clinical data, we developed a multimodal machine learning algorithm that can predict the K-AGE more accurately in people with normal Scr. This provides a novel method for a more comprehensive assessment of kidney health status in chronic kidney disease patients for future studies.

SUPPLEMENTARY DATA

Supplementary data are available at *ckj* online.

AUTHORS' CONTRIBUTIONS

Study design: L.C. and Z.H.; data acquisition: H.S. and Z.C.; CT manual segmentation: G.Z., W.S. and T.Z.; data analysis: Z.H. and Y.M.; manuscript drafting: Z.H., L.C., P.X. and X.S. All authors approved the final version of the submitted manuscript. The authors certify that neither this manuscript nor one with substantially similar content has been published or is being considered for publication elsewhere, except in abstract form.

DATA AVAILABILITY STATEMENT

The data underlying this article will be shared on reasonable request to the corresponding author.

CONFLICT OF INTEREST STATEMENT

All the authors declared no competing interests.

REFERENCES

1. Jaffe M. Ueber den Niederschlag, welchen pikrinsäure in normalem harn erzeugt und über eine neue reaction des Kreatinins. *bchm* 1886;**10**:391–400. https://doi.org/10.1515/bchm1.1886.10.5.391
2. Cockcroft DW, Gault MH. Prediction of creatinine clearance from serum creatinine. *Nephron* 1976;**16**:31–41. https://doi.org/10.1159/000180580
3. Matzke GR, Aronoff GR, Atkinson AJ, Jr *et al*. Drug dosing consideration in patients with acute and chronic kidney disease-a clinical update from Kidney Disease: Improving Global Outcomes (KDIGO). *Kidney Int* 2011;**80**:1122–37. https://doi.org/10.1038/ki.2011.322
4. Tangri N, Grams ME, Levey AS *et al*. Multinational assessment of accuracy of equations for predicting risk of kidney failure: a meta-analysis. *JAMA* 2016;**315**:164–74. https://doi.org/10.1001/jama.2015.18202
5. Tangri N, Stevens LA, Griffith J *et al*. A predictive model for progression of chronic kidney disease to kidney failure.

JAMA 2011;**305**:1553–9. https://doi.org/10.1001/jama.2011.451

6. Levey AS, Titan SM, Powe NR *et al*. Kidney disease, race, and GFR estimation. *Clin J Am Soc Nephrol* 2020;**15**:1203–12. https://doi.org/10.2215/CJN.12791019

7. Chuah LL, Miras AD, Perry LM *et al*. Measurement of glomerular filtration rate in patients undergoing obesity surgery. *BMC Nephrol* 2018;**19**:383. https://doi.org/10.1186/s12882-018-1188-7

8. Bassiony AI, Nassar MK, Shiha O *et al*. Renal changes and estimation of glomerular filtration rate using different equations in morbidly obese Egyptian patients. *Diabetes Metab Syndr* 2020;**14**:1187–93. https://doi.org/10.1016/j.dsx.2020.06.046

9. Borstnar S, Lindic J, Lezaic L *et al*. Estimation of glomerular filtration rate based on dry lean body mass in kidney transplant recipients. *Clin Nephrol* 2019;**92**:287–92. https://doi.org/10.5414/CN109882

10. Sobamowo H, Prabhakar SS. The kidney in aging: physiological changes and pathological implications. *Prog Mol Biol Transl Sci* 2017;**146**:303–40. https://doi.org/10.1016/bs.pmbts.2016.12.018

11. Korsmo MJ, Ebrahimi B, Eirin A *et al*. Magnetic resonance elastography noninvasively detects in vivo renal medullary fibrosis secondary to swine renal artery stenosis. *Invest Radiol* 2013;**48**:61–8. https://doi.org/10.1097/RLI.0b013e31827a4990

12. Asano K, Ogata A, Tanaka K *et al*. Acoustic radiation force impulse elastography of the kidneys: is shear wave velocity affected by tissue fibrosis or renal blood flow? *J Ultrasound Med* 2014;**33**:793–801. https://doi.org/10.7863/ultra.33.5.793

13. Jourde-Chiche N, Fakhouri F, Dou L *et al*. Endothelium structure and function in kidney health and disease. *Nat Rev Nephrol* 2019;**15**:87–108. https://doi.org/10.1038/s41581-018-0098-z

14. Hommos MS, Glassock RJ, Rule AD. Structural and functional changes in human kidneys with healthy aging. *J Am Soc Nephrol* 2017;**28**:2838–44. https://doi.org/10.1681/ASN.2017040421

15. Wang X, Vrtiska TJ, Avula RT *et al*. Age, kidney function, and risk factors associate differently with cortical and medullary volumes of the kidney. *Kidney Int* 2014;**85**:677–85. https://doi.org/10.1038/ki.2013.359

16. Korfiatis P, Denic A, Edwards ME *et al*. Automated segmentation of kidney cortex and medulla in CT images: a multisite evaluation study. *J Am Soc Nephrol* 2022;**33**:420–30. https://doi.org/10.1681/ASN.2021030404

17. Liu X, Chen K, Wu T *et al*. Use of multimodality imaging and artificial intelligence for diagnosis and prognosis of early stages of Alzheimer's disease. *Transl Res* 2018;**194**:56–67. https://doi.org/10.1016/j.trsl.2018.01.001

18. Abdellatif W, Ding J, Khorshed D *et al*. Unravelling the mysteries of gout by multimodality imaging. *Semin Arthritis Rheum* 2020;**50**:S17–23. https://doi.org/10.1016/j.semarthrit.2020.04.009

19. Levey AS, Stevens LA, Schmid CH *et al*. A new equation to estimate glomerular filtration rate. *Ann Intern Med* 2009;**150**:604–12. https://doi.org/10.7326/0003-4819-150-9-200905050-00006

20. Cai Q, Geng P, Li H *et al*. Semi-automatic segmentation of renal cortex and medulla based on dynamic magnetic resonance images. *2010 3rd International Conference on Biomedical Engineering and Informatics*. Yantai, China: IEEE. 2010, 555–9. https://doi.org/10.1109/BMEI.2010.5639998.

21. Couteaux V, Si-Mohamed S, Renard-Penna R *et al*. Kidney cortex segmentation in 2D CT with U-nets ensemble aggregation. *Diagn Interv Imaging* 2019;**100**:211–7. https://doi.org/10.1016/j.diii.2019.03.001

22. Li X, Chen X, Yao J *et al*. Automatic renal cortex segmentation using implicit shape registration and novel multiple surfaces graph search. *IEEE Trans Med Imaging* 2012;**31**:1849–60.

23. Mclean AJ, Cogger VC, Chong GC *et al*. Age-related pseudocapillarization of the human liver. *J Pathol* 2003;**200**:112–7. https://doi.org/10.1002/path.1328

24. Ritchie SJ, Dickie DA, Cox SR *et al*. Brain volumetric changes and cognitive ageing during the eighth decade of life. *Hum Brain Mapp* 2015;**36**:4910–25. https://doi.org/10.1002/hbm.22959

25. Horn MA. Cardiac physiology of aging: extracellular considerations. *Compr Physiol* 2015;**5**:1069–121. https://doi.org/10.1002/cphy.c140063

26. Raisi-Estabragh Z, Salih A, Gkontra P *et al*. Estimation of biological heart age using cardiovascular magnetic resonance radiomics. *Sci Rep* 2022;**12**:12805. https://doi.org/10.1038/s41598-022-16639-9

27. Nash K, Hafeez A, Hou S. Hospital-acquired renal insufficiency. *Am J Kidney Dis* 2002;**39**:930–6. https://doi.org/10.1053/ajkd.2002.32766

28. Goya C, Kilinc F, Hamidi C *et al*. Acoustic radiation force impulse imaging for evaluation of renal parenchyma elasticity in diabetic nephropathy. *AJR Am J Roentgenol* 2015;**204**:324–9. https://doi.org/10.2214/AJR.14.12493

29. Wang L, Xia P, Lv K *et al*. Assessment of renal tissue elasticity by acoustic radiation force impulse quantification with histopathological correlation: preliminary experience in chronic kidney disease. *Eur Radiol* 2014;**24**:1694–9. https://doi.org/10.1007/s00330-014-3162-5